Electrochimica Acta 106 (2013) 127–134

Contents lists available at SciVerse ScienceDirect

Electrochimica Acta

journal homepage: www.elsevier.com/locate/electacta

# Simultaneous voltammetric determination of nitrophenol isomers at ordered mesoporous carbon modified electrode

Tingting Zhang[a,b,1], Qiaolin Lang[b,1], Dapeng Yang[b], Liang Li[b], Lingxing Zeng[c], Cheng Zheng[c], Tie Li[a,*], Mingdeng Wei[c,*], Aihua Liu[b,*]

[a] College of Chemistry and Chemical Engineering, Ocean University of China, 238 Songling Road, Qingdao 266100, China
[b] Laboratory for Biosensing, Qingdao Institute of Bioenergy & Bioprocess Technology, and Key Laboratory of Bioenergy, Chinese Academy of Sciences, 189 Songling Road, Qingdao 266101, China
[c] Institute of Advanced Energy Materials, Fuzhou University, Fuzhou, Fujian 350002, China

ARTICLE INFO

*Article history:*
Received 14 April 2013
Received in revised form 11 May 2013
Accepted 15 May 2013
Available online xxx

*Keywords:*
Ordered mesoporous carbons
Voltammetric detection
Nitrophenol isomers
Simultaneous determination

ABSTRACT

In this paper, ordered mesoporous carbons (OMCs) modified glassy carbon electrode (GCE) (OMCs/GCE) was employed to investigate the electrochemical behavior of *o*-nitrophenol (*o*-NP), *m*-nitrophenol (*m*-NP) and *p*-nitrophenol (*p*-NP) in ambient–$N_2$ phosphate buffer saline. Compared with bare GCE, the OMCs/GCE exhibited obvious electrocatalytic activity towards nitrophenol isomers. The electrochemical reaction mechanism of nitrophenol at the modified electrode was also studied. At OMCs/GCE, the three nitrophenol isomers could be identified and separated successfully and the simultaneous determination was realized by detecting the reduction peaks of their intermediate products (at 0.209 V vs. saturated calomel electrode for *p*-NP, 0.020 V for *m*-NP and −0.201 V for *o*-NP) with differential pulse voltammetry. Under the optimized experimental conditions, the linear ranges of the calibration curves were 2–90 μM for *p*-NP, 1–100 μM for *m*-NP and 0.5–90 μM for *o*-NP with limits of detection of 0.1 μM, 0.06 μM and 0.08 μM for *p*-NP, *m*-NP and *o*-NP, respectively (S/N = 3). Therefore, the proposed method is simple, rapid, stable, sensitive, specific, reproducible and cost-effective, which can be applicable for real samples detection.



## 1. Introduction

It has been reported that *o*-nitrophenol (*o*-NP), *m*-NP, and *p*-NP are three important environmental pollutants and they are classified as the hazardous wastes and priority toxic pollutants by Environmental Protection Agency of America [1,2]. These compounds are poisonous to human and animals, which would result in severe diseases, such as methemoglobinemia, fervescence, damage of liver and kidney [3–6]. Nitrophenol isomers are also harmful to plants, for instance, irrigating crops with water which contains nitrophenol isomers over 0.7 mM will lead to the reduction of output [7]. The three isomers are widely used in industrial production of pharmaceuticals, dyes and pesticides [8–10], therefore, they broadly distribute in soil and aquatic environment, and are difficult to degrade because of high stability [11–14]. For above-mentioned reasons, their detection becomes one of the important projects for environmental analysis. On the other hand, due to their similar structures and properties, the three isomers usually coexist and interfere with each other during determination. At present, many experimental methods have been developed for the simultaneous determination of nitrophenol isomers, for example, flow injection analysis [15], spectrophotometry [16,17], high performance liquid chromatography [18], capillary electrophoresis [19]. However, these approaches are complex in sample preparation and generally need expensive instrumentation. Moreover, the on-site inspection is very difficult. Therefore, it is very important to explore a simple, rapid and cost-effective method for their simultaneous determination.

The emerging nanotechnology has opened up new exciting avenues for offering great opportunities for analytical applications, mostly due to the extraordinary physical and chemical properties of nanostructured materials [20–27]. In recent years, electrochemical method has attracted much attention due to its high-efficiency, low-cost, and easy-to-operation. Up to now, several kinds of nanomaterial-modified electrodes for simultaneous determination of nitrophenol isomers have been reported, for instance, multiwalled carbon nanotubes (MWNTs) modified glassy carbon electrode (GCE) (MWNTs/GCE) using linear sweep voltammetry (LSV) [28], nano-gold (nano-Au) modified GCE (nano-Au/GCE) using semi-derivative voltammetry (SDV) [5], β-cyclodextrin (CD)

* Corresponding authors. Tel.: +86 532 80662758; fax: +86 532 80662778.
*E-mail addresses:* litie@ouc.edu.cn (T. Li), wei-mingdeng@fzu.edu.cn (M. Wei), liuah@qibebt.ac.cn (A. Liu).
[1] These two authors contributed equally to this work.

0013-4686/$ – see front matter © 2013 Elsevier Ltd. All rights reserved.
http://dx.doi.org/10.1016/j.electacta.2013.05.055

functionalized reduced graphene oxide (RGO) modified GCE (CD-RCO/GCE) using differential pulse voltammetry (DPV) [12], and CD functionalized mesoporous silica (SBA) modified carbon paste electrode (CPE) (CD-SBA/CPE) [2]. However, these methods either lack sensitivity, or are complicated in preparation of the electrodes.

Since the discovery of ordered mesoporous carbons (OMCs) in 1999, many scientists have paid great attention to the development of this kind carbon material due to its large surface area, well-defined pore size, and flexible framework [29–31]. It has been reported that largely due to the existence of the edge plane-like defective site and oxygen-containing functional groups on the surface of OMCs, they can provide a great deal of favorable sites to transmit electrons for electroactive substances [3,32]. At present, this ordered carbon material has been widely used in sensing, energy storage, bioreactor construction and catalytic application [32]. The advantages of fast electron transfer, high thermal stability and excellent electrocatalytic activity suggest that the OMCs will be a promising candidate for electrode modified material.

In this paper, we systematically studied the electrochemistry of nitrophenol isomers at OMCs-modified electrode. It turned out that the OMCs-modified electrode exhibited excellent electrocatalytic activity towards nitrophenol isomers. Well-separated voltmometric peaks were observed in their mixture solution, which could be applicable to simultaneously detect the three nitrophenol isomers.

## 2. Materials and methods

### 2.1. Chemicals and reagents

Triblock copolymer of Pluronic (P123) and Nafion (perfluorinated ion-exchange resin, 5 wt% solution in a mixture of lower aliphatic alcohols and water) were purchased from Aldrich Corporation. Tetraethoxysilane (TEOS) was purchased from Sinopharm Chemical Reagent Corporation. *o*-NP, *m*-NP and *p*-NP were purchased from Xiya Reagent Corporation, China and used without further purification. The solid nitrophenol isomers should be stored in the cool and dry place to avoid direct sunlight and their solutions should be prepared immediately before used. Phosphate buffer saline (PBS) was used as the supporting electrolyte. All other reagents were of the highest grade and all solutions were prepared with ultrapure water.

### 2.2. Synthesis of ordered mesoporous carbons

OMCs were synthesized according to the literatures with modification [29–31]. Initially, 2.0 g of P123 was added into 80 g of distilled water containing 60 g of 2 M HCl, and then the mixture was adequately stirred at 35 °C until P123 was completely dissolved. Following that, 4.2 g of TEOS was injected into the mixture, and stirred for 20 h at 35 °C. Subsequently, the mixture was aged at 100 °C overnight. The products were obtained by filtration and dried in air for 2 h. Next, the as-prepared precipitate was added into a mixture containing 1.5 g sucrose, 0.17 g $H_2SO_4$ and 10 g $H_2O$. After adequately stirring, the suspension was heated for 6 h at 100 °C in an oven, followed by continuously heating for 6 h at 160 °C. Afterwards, the brown product was calcined in a tubular furnace for 5 h at 550 °C and for 3 h at 900 °C under the protection of nitrogen gas in turn. Finally, OMCs was formed via the addition of 1.0 M NaOH into the resulting suspension. The obtained OMCs by centrifugation was washed, dried at 80 °C, and stored in a drier.

### 2.3. Preparation of OMCs modified electrode

The glassy carbon electrode (3 mm in diameter) was polished successively with 0.3 and 0.05 μm alumina slurry and sonicated in anhydrous ethanol and ultrapure water for 3 min, respectively [33]. Then, the electrode was thoroughly rinsed with ultrapure water. Nafion-OMCs composite was prepared by mixing 1.0 mL Nafion (0.05 wt%) with 2.0 mg OMCs powder and sonicated until a homogeneous aqueous dispersion resulted. 8.0 μL of the mixture was dropped onto the inverted electrode and dried under room temperature to acquire OMCs film modified GCE. At last, 4.0 μL of Nafion (0.05 wt%) was syringed onto the surface of modified electrode. Before use, the modified electrode was immersed into ultrapure water to remove any loosely bound modifiers.

### 2.4. Apparatus and methods

The wide-angle X-ray diffraction (XRD) patterns were recorded on a PANalytical X'Pert spectrometer using the Co Kα radiation (λ = 1.789 Å), and the data would be changed to Cu Kα data. Transmission electron micrograph (TEM) was taken on a FEI F20 S-TWIN instrument. $N_2$ adsorption–desorption analysis was measured on a Micromeritics ASAP 2020 instrument, pore volumes were determined using the adsorbed volume at a relative pressure of 0.99, multipoint Brunauer–Emmet–Teller (BET) surface area was estimated from the relative pressure range from 0.06 to 0.3. The pore size distributions of the as-prepared samples were analyzed using the Barrett–Joyner–Halenda (BJH) method. The electrochemical experiments were performed with CHI660D electrochemical workstation (CH Instruments, Chenhua, Shanghai, China). All electrochemical experiments were carried out in a conventional three-electrode system using a bare GCE or a modified GCE as working electrode, a platinum wire as counter electrode and a saturated calomel electrode (SCE) as reference electrode. All potentials in this article were recorded versus this reference. All measurements were performed at room temperature (~23 °C). The PBS solution was deaerated with high purity nitrogen for 20 min previously and kept on feeding nitrogen through the whole experimental process.

## 3. Results and discussion

### 3.1. Characherization of prepared OMCs

The TEM image of the prepared OMCs along the [0 0 1] direction demonstrates the regular pattern of carbon particles in the mesopore channel structure (Fig. 1). For mesoporous carbon, the BET surface area and pore volume are 1158 $m^2 g^{-1}$ and 1.26 $cm^3 g^{-1}$, respectively. $N_2$ adsorption-desorption isotherm showed the pore with an average pore diameter of approximately 3.9 nm (Fig. 2).

### 3.2. Electrochemical behavior and reaction mechanism of nitrophenol isomers at OMCs/GCE

The cyclic voltammograms (CVs) of *p*-NP, *m*-NP and *o*-NP (each 10 μM) at bare GCE and OMCs/GCE in 0.1 M PBS (pH 4.8) buffer under saturated-$N_2$ are shown in Fig. 3. At bare GCE, *p*-NP, *m*-NP and *o*-NP gave a reduction peak at −0.731 V, −0.669 V and −0.623 V, respectively (curves a of Fig. 3A–C), which related to the irreversible reduction of nitryl [34,35]. Meanwhile, at OMCs/GCE, *p*-NP, *m*-NP and *o*-NP exhibited a clear nitryl reduction peak at −0.639 V, −0.582 V and −0.573 V, respectively (curves c of Fig. 3A–C). After modified with OMCs, the background current increased obviously, furthermore, the current signal increased significantly and all the reduction peak potentials positively shifted. To illustrate the other features at OMCs/GCE, *p*-NP was taken as an example. Besides the clear reduction peak of nitryl, a new pair of well-defined redox peaks appeared with oxidation and reduction peak at 0.239 V and 0.209 V at OMCs/GCE (Fig. 3A, curve c). Compared to the blank controlled trial (Fig. 3A, curve b), this new pair of peaks are attributed to the electrochemical behavior of *p*-NP rather than OMCs.Similarly,

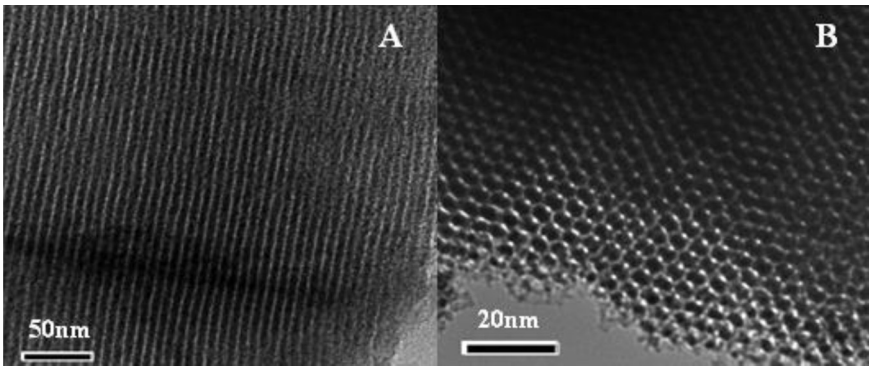


**Fig. 1.** (A) TEM image showing mesopore channel structure. (B) TEM image of the mesoporous carbon along the [0 0 1] direction.

a new pair of redox peaks of *m*-NP could be obtained at 0.082 V and 0.020 V (Fig. 3B, curve c), and that of *o*-NP were observed at −0.153 V and −0.201 V (Fig. 3C, curve c), revealing that the modified electrode exhibited nice electrocatalytic activity towards nitrophenol isomers. The plenty of edge plane-like defects and oxygen-containing functional groups on the surface of OMCs would provide lots of favorable sites for electron transfer, and the well-defined pore size showed different space resistances to different substances, which make a difference to the rate of nitrophenol isomers to the electrode surface [3]. In addition, unlike the other two isomers, *o*-NP also showed an oxidation peak at 0.324 V, and according to the relevant literature, this peak should be resulted from the oxidation of phenolic hydroxyl [36–38]. In order to evaluate the feasibility of OMCs/GCE for the simultaneous determination of nitrophenol isomers, the electrochemical behavior of mixed components (each 10 μM) were investigated. At bare GCE, there was only one broad reduction peak of nitryl at approximate −0.680 V (Fig. 3D, curve a), so it was impossible to use bare GCE for the simultaneous determination. However, at OMCs/GCE, besides the broad reduction peak around −0.620 V, three well-defined redox peaks could be recognized accurately (Fig. 3D, curve c). Thus, the *o*-, *m*-, and *p*-NP could be well separated and the simultaneous determination was feasible at OMCs/GCE. Furthermore, the pairs of redox peaks of nitrophenol isomers in the mixture solution appeared at the same positions as in the individual solution, which proved that their redox behavior in the mixture solution proceeded independently.

To illustrate the electrochemical mechanism, continuous CV measurements of three nitrophenol isomers mixture at OMCs/GCE were tested. As shown in Fig. 4, during the first cycle, only one broad reduction peak of nitryl ($c_1$) appeared in the cathodic sweep, while in the anodic sweep four oxidation peaks emerged at −0.153 V ($a_2$), 0.082 V ($a_3$), 0.239 V ($a_4$) and 0.324 V ($a_{(-OH)}$) in sequence. Different from the first cycle, in the second cycle, in addition to the reduction peak of nitryl, three new reduction peaks ($c_4$, $c_3$, $c_2$) appeared at 0.209 V, 0.020 V and −0.201 V in sequence in the cathodic sweep, which were corresponded to $a_4$, $a_3$ and $a_2$. Clearly, the emergence of the three reduction peaks was accompanied by the drop of reduction peak of nitryl group, and they would become stable finally after the following successive cyclic sweeps. To further make clear the origination of the three redox pairs, the potential range was changed into −0.4–0.6 V in which range the reduction potential of nitryl group was not reached and it could not be reduced. CV of nitrophenol isomers mixture in this potential showed that the three couples did not appear, either. So it was apparent that the three peak couples ($a_2/c_2$, $a_3/c_3$, $a_4/c_4$) are derived from the intermediate products of nitryl group reduction.

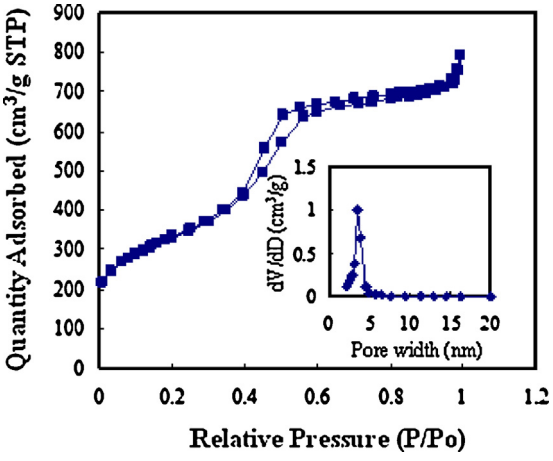


**Fig. 2.** $N_2$ adsorption–desorption isotherms of the prepared OMCs. Inset: pore size distribution from the desorption branch through the BJH method.

According to the original reaction process proposed by previous literatures (Scheme 1) [39,40], in the first step, nitrophenol is reduced to hydroxyl aminophenol along with four electrons and four protons transfer and the reduction peak of nitryl ($c_1$) derived from this stage. Then, the hydroxyl aminophenol would remove one $H_2O$ and change to benzoquinoneimine, which can lose two electrons to form aminophenol finally [41]. Analyzed from above results, the reaction is interrupted at hydroxyl aminophenol stage at OMCs/GCE in this work, hydroxyl aminophenol can be captured by the well-defined pore and oxidized at the catalytic active site of OMCs to nitrosophenol which is a reversible reaction with two electrons and two protons transfering, and this is the origin of $a_2/c_2$, $a_3/c_3$ and $a_4/c_4$ (Scheme 2). As *o*-NP also showed an oxidation peak at 0.324 V ($a_{(-OH)}$) resulting from phenolic hydroxyl, the nitrosophenol reductive peaks ($c_2$, $c_3$, $c_4$) as the study peaks were studied to avoid unnecessary interference between $a_{(-OH)}$ and $a_4$ and simplify the procedure of simultaneous determination.

### 3.3. Optimization of experimental conditions

#### 3.3.1. Effect of solution pH

As proton participates in the electrode reaction, the acidity of electrolyte has a remarkable effect on the electrochemical behavior of nitrophenol isomers. Here the cathodic peak was studied. As buffer pH was increased from 4.0 to 9.0, the cathodic current of three nitrophenol isomers showed similar trend (Fig. 5A). That is, the current response climbed up first and reached to the maximum at pH 5.0, then declined significantly. Meanwhile, with the increase of pH, the peak potential of three nitrophenol isomers all shifted negatively and showed linear relationship with pH (Fig. 5B). The linear regression equations were $E_{pc}$ (*p*-NP) = −0.057

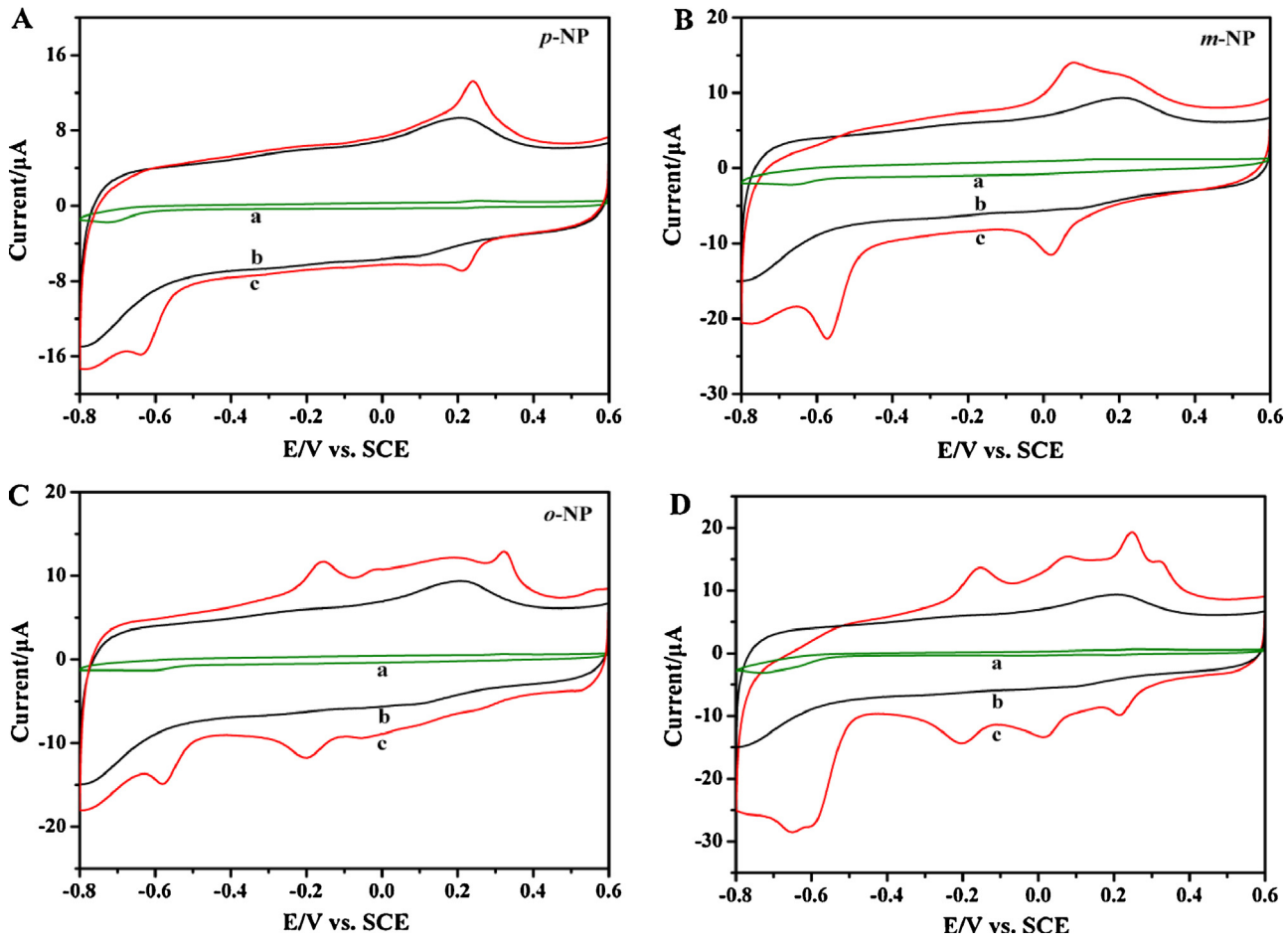


**Fig. 3.** CVs of (A) *p*-NP, (B) *m*-NP, (C) *o*-NP (each 10 μM) and (D) mixture of three isomers at bare GCE (a) and OMCs/GCE (c). CV of 0.1 M PBS (pH 4.8) solution at OMCs/GCE (b). Scan rate, 50 mV/s.

pH + 0.479, $R = 0.9978$; $E_{pc}$ (*m*-NP) = −0.061 pH + 0.316, $R = 0.9976$; $E_{pc}$ (*o*-NP) = −0.056 pH + 0.066, $R = 0.9940$, According to Eq. (1) [2]:

$$\frac{dE_p}{dpH} = -2.303\frac{mRT}{nF} \quad (1)$$

where *m* and *n* refer to the transferring number of proton and electron, respectively. The value of *m*/*n* in this reaction was calculated to be 1.05 (*p*-NP), 0.98 (*m*-NP), 0.96 (*o*-NP) and all equalled to 1.0 approximately, indicating that the transferring number of proton and electron was same. This result agrees with the reported conclusion that the nitrosophenol is reduced to hydroxyl aminophenol with two electrons and two protons transferring. When pH > 6, the peaks became wider and inconspicuous, indicating that the reaction became weaker and weaker along with the increase of pH value. Then CVs of the modified electrode in nitrophenol isomers with different pH values of 4.5, 4.8, 5.2 and 5.5 were compared. The peaks were relatively larger and sharper at pH 4.8. So PBS buffer with pH 4.8 was chosen in this study.

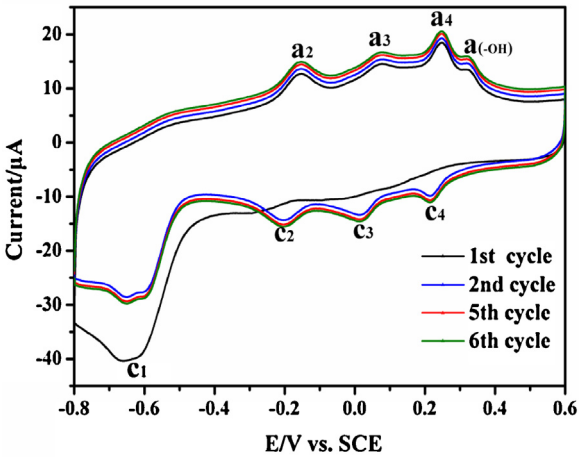


**Fig. 4.** Continuous CV measurement of nitrophenol isomers mixture (each 10 μM) at OMCs/GCE. Scan rate, 50 mV/s.

### 3.3.2. *Effect of scan rate*

The effect of scan rate on CV responses of three nitrophenol isomers at OMCs/GCE was studied. Both the oxidation peaks and reduction peaks enhanced with the increase of scan rate, while the peak potential remained almost unchanged (Fig. 6). The reduction peak current of nitrosophenol exhibited linearly proportional to the square root of scan rate in the range of 10–250 mV/s, suggesting that the reduction of nitrosophenol at OMCs/GCE was a diffusion-controlled process.

### 3.4. *Simultaneous determination of nitrophenol isomers*

On the basis of CV results described above, the simultaneous determination of nitrophenol isomers could be achieved at OMCs/GCE. DPV was used to investigate the simultaneous determination with the changing concentration of one isomer continually

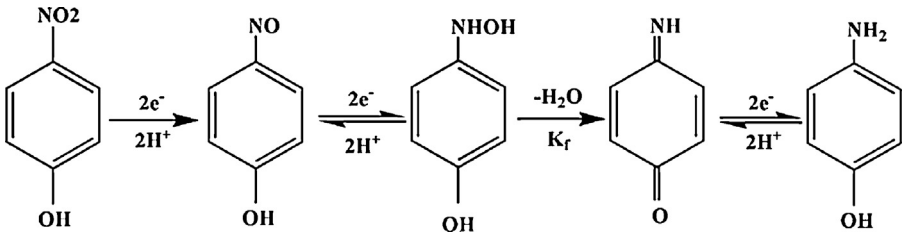


**Scheme 1.** The reaction mechanism of nitrophenol in previous literatures [39,40].

and the other two keeping at constant values. The three nitrophenol isomers were fixed at different concentrations because of their different current response at OMCs/GCE. Taking *p*-NP as an example, the $i_{pc}$ value increased and the peak became shaper with the increase of concentration of *p*-NP in the presence of the other two isomers (Fig. 7A). However, a plateau appeared when *p*-NP was higher than 90 μM, which were probably originating from the intermediate products (nitrosophenol) reaching saturated adsorption at the surface of OMCs/GCE. The $i_{pc}$ was linear with concentration of *p*-NP in the range of 2–90 μM and the linear regression equation was $i_{pc}$ (*p*-NP) = −0.156 Conc + 0.018 with a regression coefficient (*R*) of 0.9970. The other two isomers showed similar results that *m*-NP and *o*-NP reached saturated adsorption at 100 and 90 μM, respectively. The linear ranges towards *m*-NP and *o*-NP were 1–100 μM and 0.5–90 μM and the linear regression equations were $i_{pc}$ (*m*-NP) = −0.271 Conc −1.588 with *R* = 0.9979; $i_{pc}$ (*o*-NP) = −0.296 Conc + 0.119 with *R* = 0.9988. The limit of detections (LOD) of *p*-NP, *m*-NP and *o*-NP were evaluated to be 0.1, 0.06 and 0.08 μM, respectively (S/N = 3). Several kinds of modified electrodes were reported for simultaneous determination of nitrophenol isomers, and the performances of these electrodes are summarized in Table 1. Obviously, compared with CD-RGO/GCE [12], the OMCs/GCE showed wider liner range and much lower detection limits. Although both the nano-Au/GCE [5] and MWNTs/GCE [42] provided broad liner range, LOD values were high. Interestingly, CD-SBA/CPE was also reported for simultaneous detection of nitrophenol isomers with relatively low LODs, but the dynamic linear range was narrow [2], in which the average pore diameter of SBA was 4.4 nm, a little larger than the pore size of 3.9 nm for our OMCs. However, both functionalized mesoporous silica with β-CD and the followed carbon paste electrode were complex and cockamamie [2]. In our case, the preparation of OMCs/GCE was simple without additional inclusion of functional materials.

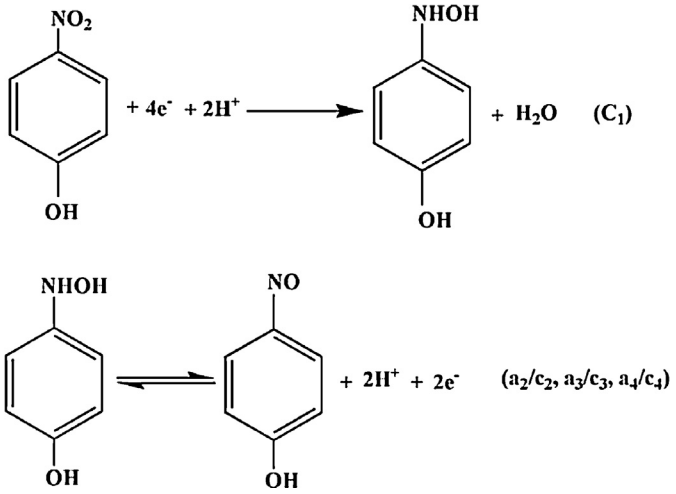


**Scheme 2.** The electrochemical reaction mechanism at OMCs/GCE.

Furthermore, the OMCs/GCE is fairly stable and feasible for the detection of real samples.

### 3.5. Stability of OMCs/GCE

A consecutive CV measurement was carried out to test the operational stability of OMCs/GCE. The peak currents of all the three nitrophenol isomers retained over 95% of their initial values and without obvious potential shift after continuous 90 circles, indicating that the modified electrode exhibited good operational stability. The long-term stability of the modified electrode was also evaluated. The current response was measured every two days in the mixture of the three nitrophenol isomers (each 10 μM). The modified electrode was stored in 4 °C refrigerator when it was not in

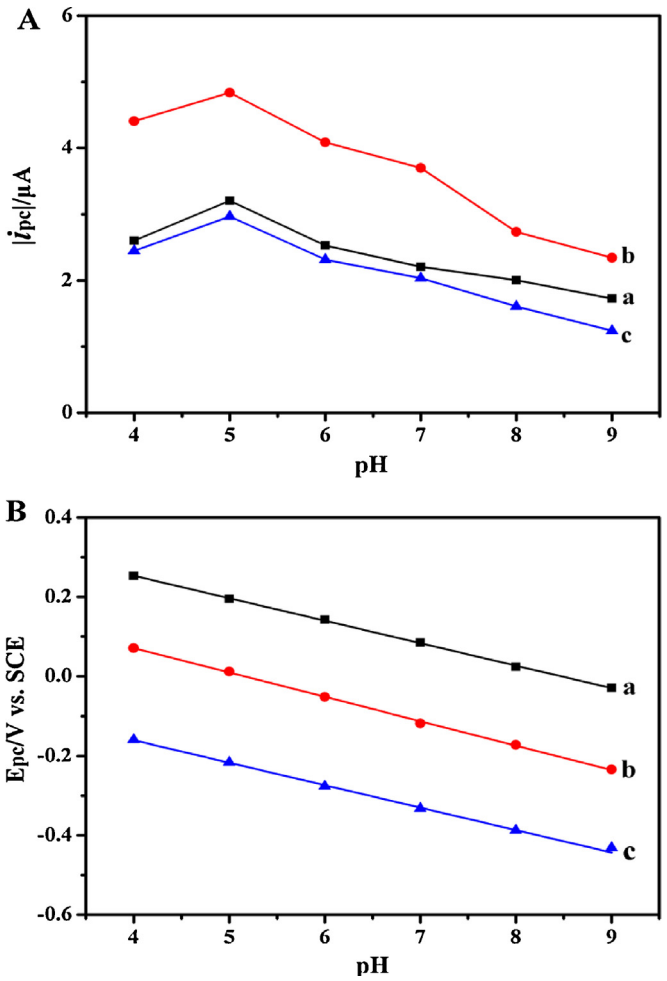


**Fig. 5.** (A) The relationship between pH and absolute value of cathodic peak current ($|i_{pc}|$). (B) The cathodic peak potential as a function of buffer pH. *p*-NP (a), *m*-NP (b), *o*-NP (c). CVs were measured in 10 μM nitropenol isomer solution varying buffer pH. Scan rate, 50 mV/s.

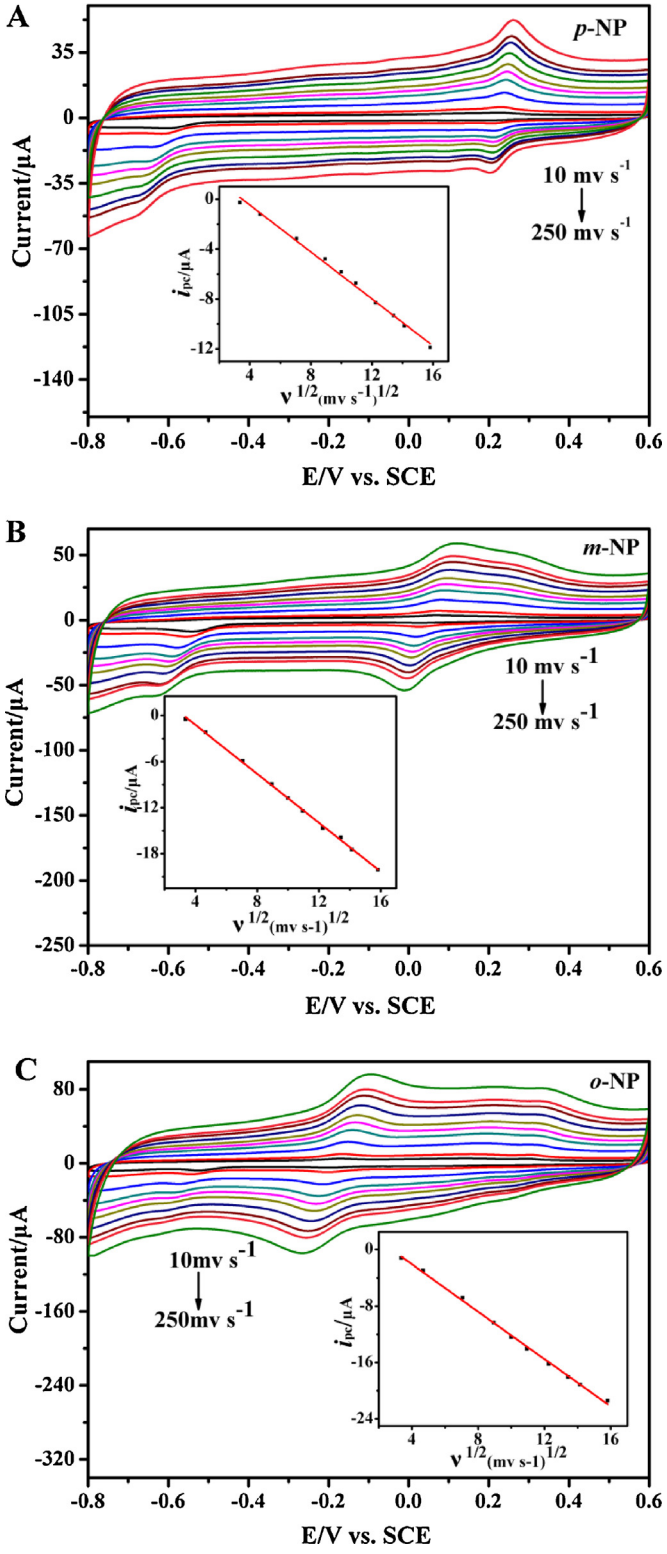


**Fig. 6.** CVs of nitrophenol isomers at OMCs/GCE at different scan rates. *p*-NP (A), *m*-NP (B), *o*-NP (C), (with concentration of 10 μM). Inset: The relationship between the $i_{pc}$ values and the square root of scan rate.

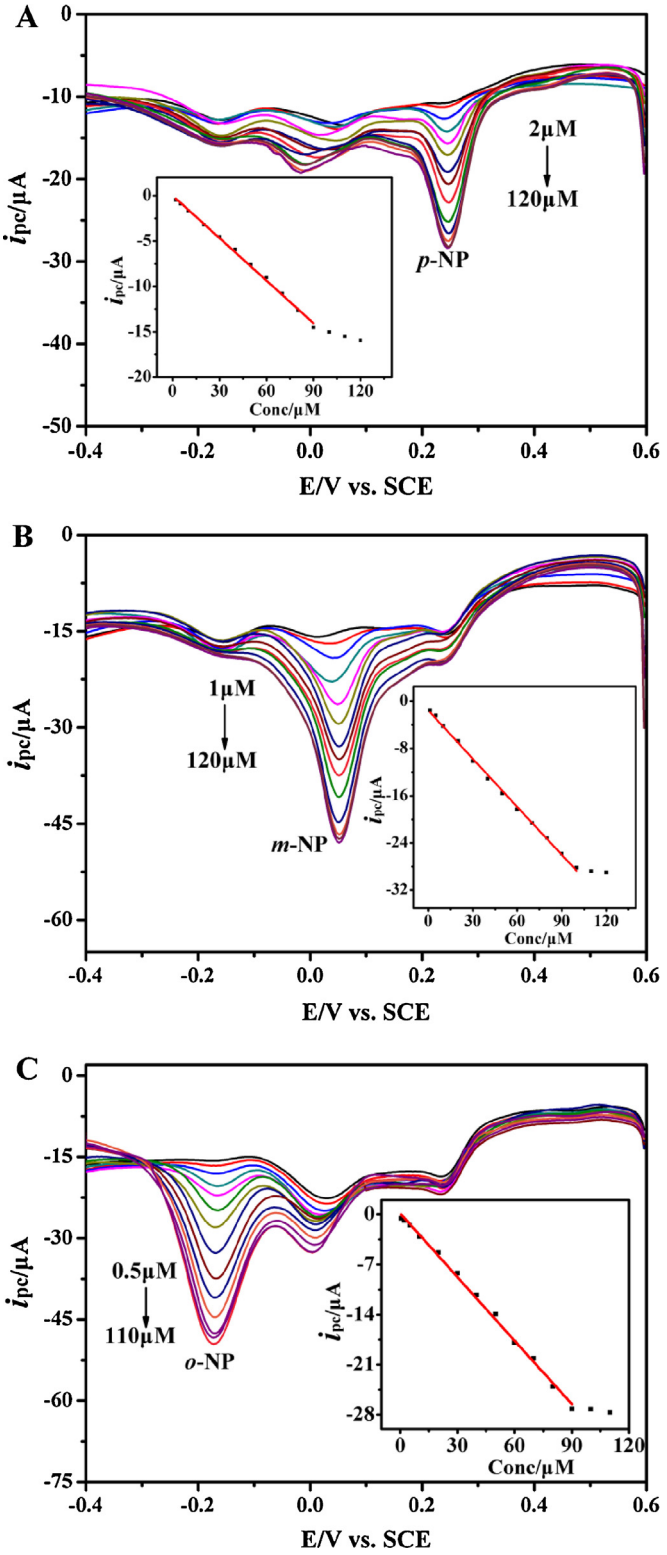


**Fig. 7.** DPV responses of nitrophenol isomers at OMCs/GCE in 0.1 M PBS (pH 4.8). (A) *m*-NP and *o*-NP were fixed at 5 μM, varying *p*-NP concentrations (2, 5, 10, 20, 30, 40, 50, 60, 70, 80, 90, 100, 110, 120 μM). (B) *p*-NP and *o*-NP were fixed at 10 and 5 μM, respectively, varying *m*-NP concentrations (1, 5, 10, 20, 30, 40, 50, 60, 70, 80, 90, 100, 110, 120 μM). (C) *p*-NP and *m*-NP were fixed at 10 and 5 μM, respectively, varying *m*-NP concentrations (0.5, 2, 5, 10, 20, 30, 40, 50, 60, 70, 80, 90, 100, 110 μM). Inset: the calibration curve between $i_{pc}$ and the concentration of *p*-NP, *m*-NP, *o*-NP. Scan rate, 50 mV/s.

**Table 1**
Comparison of performances of OMCs/GCE with other modified electrodes reported so far.

| Modified electrode | Method | Performance | *p*-NP | *m*-NP | *o*-NP | Ref |
|---|---|---|---|---|---|---|
| CD-RGO/GCE | DPV | Liner range (μM) | 7.0–70 | 7.0–43 | 7.0–64 | [12] |
| | | LOD (μM) | 0.36 | 0.7 | 0.14 | |
| CD-SBA/CPE | DPV | Liner range (μM) | 2–14 | 2–16 | 2–14 | [2] |
| | | LOD (μM) | 0.1 | 0.05 | 0.1 | |
| Nano-Au/GCE | SDV | Liner range (μM) | 50–1000 | 50–2000 | 50–1000 | [5] |
| | | LOD (μM) | 8.0 | 5.0 | 8.0 | |
| MWNTs/GCE | LSV | Liner range (μM) | 4.0–200 | 10–100 | 2.0–400 | [42] |
| | | LOD (μM) | 0.4 | 6.0 | 0.5 | |
| OMCs/GCE | DPV | Liner range (μM) | 2.0–90 | 1.0–100 | 0.5–100 | This work |
| | | LOD (μM) | 0.1 | 0.06 | 0.08 | |

**Table 2**
Determination of *p*-NP, *m*-NP, and *o*-NP in real samples.

| | Tap water | | | Sea water | | | Waste water | | |
|---|---|---|---|---|---|---|---|---|---|
| | *p*-NP | *m*-NP | *o*-NP | *p*-NP | *m*-NP | *o*-NP | *p*-NP | *m*-NP | *o*-NP |
| Conc. (μM) | – | – | – | – | – | – | – | 7.83 | 8.11 |
| Added (μM) | 10.00 | 10.00 | 10.00 | 10.00 | 10.00 | 10.00 | 10.00 | 10.00 | 10.00 |
| Found (μM) | 9.74 | 10.21 | 9.82 | 9.88 | 10.17 | 10.06 | 9.72 | 18.24 | 17.95 |
| RSD (% $n = 6$) | 2.8 | 3.1 | 2.5 | 3.0 | 2.7 | 2.3 | 2.4 | 3.2 | 2.6 |
| Recovery (%) | 97.4 | 102.1 | 98.2 | 98.8 | 101.7 | 100.6 | 97.2 | 104.1 | 98.4 |

use. During the beginning of three weeks, there was no apparent decrease of the current response. After that, the current response began to decrease gradually. However, one month later the current signals still remained 77% initial response for *p*-NP and 75% for *m*-NP and 81% for *o*-NP.

### 3.6. Selectivity of the modified electrode

The possible interferences from some kinds of inorganic ions and organic compounds on the detection of nitrophenol isomers with the OMCs/GCE were studied. The $i_{pc}$ of each nitrosophenol isomer in the presence of of other species was measured for three times. If the $i_{pc}$ change was less than ±5% in the presence of other species, it would be considered that there was no interference on the detection of nitrophenol isomers [43,44]. A great number of cations such as $Al^{3+}$, $Cu^{2+}$, $Ca^{2+}$, $Zn^{2+}$, $Mg^{2+}$ and anions such as $NO_3^-$, $Br^-$, $SO_4^{2-}$ and $Ac^-$ (each 1 mM) were added into the mixture of nitrophenol isomers (each 10 μM), separately. It turned out that 100-fold excess of these ions had no effect on the determination of 10 μM nitrophenol isomers. Similarly, organic compounds including phenol, benzene, toluene, *p*-cresol, *m*-cresol, *o*-cresol, chlorophenol, catechol, resorcinol, hydroquinone, *p*-hydroxybenzoic acid, *m*-hydroxybenzoic acid, salicylic acid, and 2, 6-di-tert-butyl-4-methylphenol (each 100 μM) had not effecton the detection of 10 μM nitrophenol isomers. Therefore, common inorganic ions and organic compounds had no influence on the signals of nitrophenol isomers.

### 3.7. Real samples detection

To study the applicability of OMCs/GCE, tap water, seawater and wastewater were measured as the real samples. The sample solutions were first filtered through a 0.22 μm membrane, and the filtrate was collected. Before measurement, the ionic strength and pH of the real sample solution should be adjusted to match with PBS buffer. The recovery of this method was investigated by standard-addition method. Each of the samples was measured for six times. As the results listed in Table 2, the recoveries are between 95% and 105%, so the proposed method was feasible for the detection of real samples.

## 4. Conclusions

The OMCs modified GCE (OMCs/GCE) was developed to study the electrochemical behavior of nitrophenol isomers. Compared with bare GCE, the OMCs/GCE exhibited enhanced electrocatalytic activity towards nitrophenol isomers. At OMCs/GCE, the three nitrophenol isomers could be identified and separated successfully and the simultaneous determination was realized by detecting the reduction peaks of their intermediate products (at 0.209 V for *p*-NP, 0.020 V for *m*-NP and −0.201 V for *o*-NP) with differential pulse voltammetry. Under the optimized experimental conditions, the linear ranges of the calibration curves were 2–90 μM for *p*-NP, 1–100 μM for *m*-NP and 0.5–90 μM for *o*-NP, which could be applicable for real samples determination. Thus, a sensitive, selective and reproducible and cost-effective electroanalytical method was developed for the discrimination and measurement of nitrophenol isomers, which holds great potential in the wastewater monitoring system and other in situ environment monitoring.

## Acknowledgements

This work was financially supported by National Natural Science Foundation of China (Nos. 21173049, 31200598, and 21275152), National Science Foundation for Fostering Talents in Basic Research of National Natural Science Foundation of China (J1103303, J2012-029) and the Hundred-Talent-Project (No. KSCX2-YW-BR-7),Chinese Academy of Sciences.

## References

[1] K. Asadpour-Zeynali, P. Najafi-Marandi, Bismuth modified disposable pencil-lead electrode for simultaneous determination of 2-nitrophenol and 4-nitrophenol by net analyte signal standard addition method, Electroanalysis 23 (2011) 2241.
[2] X. Xu, Z. Liu, X. Zhang, S. Duan, S. Xu, C. Zhou, β-Cyclodextrin functionalized mesoporous silica for electrochemical selective sensor: simultaneous determination of nitrophenol isomers, Electrochimica Acta 58 (2011) 142.
[3] J. Bai, L. Guo, J.C. Ndamanisha, B. Qi, Electrochemical properties and simultaneous determination of dihydroxybenzene isomers at ordered mesoporous carbon-modified electrode, Journal of Applied Electrochemistry 39 (2009) 2497.
[4] M.A. El Mhammedi, M. Achak, M. Bakasse, A. Chtaini, Electrochemical determination of para-nitrophenol at apatite-modified carbon paste electrode:

application in river water samples, Journal of Hazardous Materials 163 (2009) 323.
[5] L. Chu, L. Han, X. Zhang, Electrochemical simultaneous determination of nitrophenol isomers at nano-gold modified glassy carbon electrode, Journal of Applied Electrochemistry 41 (2011) 687.
[6] C. Yang, Electrochemical determination of 4-nitrophenol using a single-wall carbon nanotube film-coated glassy carbon electrode, Microchimica Acta 148 (2004) 87.
[7] R. de Cassia Silva Luz, F.S. Damos, A.B. de Oliveira, J. Beck, L.T. Kubota, Voltammetric determination of 4-nitrophenol at a lithium tetracyanoethylenide (LiTCNE) modified glassy carbon electrode, Talanta 64 (2004) 935.
[8] K.C. Honeychurch, J.P. Hart, Voltammetric behavior of p-nitrophenol and its trace determination in human urine by liquid chromatography with a dual reductive mode electrochemical detection system, Electroanalysis 19 (2007) 2176.
[9] W. Zhang, J. Chang, J. Chen, F. Xu, F. Wang, K. Jiang, Z. Gao, Graphene–Au composite sensor for electrochemical detection of para-nitrophenol, Research on Chemical Intermediates 38 (2012) 2443.
[10] J. Li, D. Kuang, Y. Feng, F. Zhang, Z. Xu, M. Liu, A graphene oxide-based electrochemical sensor for sensitive determination of 4-nitrophenol, Journal of Hazardous Materials 201–202 (2012) 250.
[11] K. Asadpour-Zeynali, P. Soheili-Azad, Simultaneous polarographic determination of 2-nitrophenol and 4-nitrophenol by differential pulse polarography method and support vector regression, Environmental Monitoring and Assessment 184 (2012) 1089.
[12] Z. Liu, X. Ma, H. Zhang, W. Lu, H. Ma, S. Hou, Simultaneous determination of nitrophenol Isomers based on β-cyclodextrin functionalized reduced graphene oxide, Electroanalysis 24 (2012) 1178.
[13] Z. Liu, J. Du, C. Qiu, L. Huang, H. Ma, D. Shen, Y. Ding, Electrochemical sensor for detection of p-nitrophenol based on nanoporous gold, Electrochemistry Communications 11 (2009) 1365.
[14] A.K. Kafi, A. Chen, A novel amperometric biosensor for the detection of nitrophenol, Talanta 79 (2009) 97.
[15] M. Miró, A. Cladera, J.M. Estela, V.ı. Cerdà, Dual wetting-film multi-syringe flow injection analysis extraction application to the simultaneous determination of nitrophenols, Analytica Chimica Acta 438 (2001) 103.
[16] D.A. Perry, H.J. Son, J.S. Cordova, L.G. Smith, A.S. Biris, Adsorption analysis of nitrophenol isomers on silver nanostructures by surface-enhanced spectroscopy, Journal of Colloid and Interface Science 342 (2010) 311.
[17] A. Niazi, A. Yazdanipour, Spectrophotometric simultaneous determination of nitrophenol isomers by orthogonal signal correction and partial least squares, Journal of Hazardous Materials 146 (2007) 421.
[18] R. Belloli, B. Barletta, E. Bolzacchini, S. Meinardi, M. Orlandi, B. Rindone, Determination of toxic nitrophenols in the atmosphere by high-performance liquid chromatography, Journal of Chromatography A 846 (1999) 277.
[19] X. Guo, Z. Wang, S. Zhou, The separation and determination of nitrophenol isomers by high-performance capillary zone electrophoresis, Talanta 64 (2004) 135.
[20] M. Curreli, C. Li, Y. Sun, B. Lei, M.A. Gundersen, M.E. Thompson, C. Zhou, Selective functionalization of $In_2O_3$ nanowire mat devices for biosensing applications, Journal of the American Chemical Society 127 (2005) 6922.
[21] A. Liu, M. Wei, I. Honma, H. Zhou, Direct electrochemistry of myoglobin in titanate nanotubes film, Analytical Chemistry 77 (2005) 8068.
[22] F. Patolsky, G. Zheng, C.M. Lieber, Nanowire-based biosensors, Analytical Chemistry 78 (2006) 4260.
[23] A. Liu, M.D. Wei, I. Honma, H. Zhou, Biosensing properties of titanate-nanotube films: selective detection of dopamine in the presence of ascorbate and uric acid, Advanced Functional Materials 16 (2006) 371.
[24] A. Liu, I. Honma, H. Zhou, Simultaneous voltammetric detection of dopamine and uric acid at their physiological level in the presence of ascorbic acid using poly(acrylic acid)-multiwalled carbon-nanotube composite-covered glassy-carbon electrode, Biosensors and Bioelectronics 23 (2007) 74.
[25] A. Liu, H. Zhou, I. Honma, M. Ichihara, Switchable titanate-nanotube electrode sensitive to nitrate, Applied Physics Letters 90 (2007) 253112.
[26] A. Liu, Towards development of chemosensors and biosensors with metal-oxide-based nanowires or nanotubes, Biosensors and Bioelectronics 24 (2008) 167.
[27] E. Stern, J.F. Klemic, D.A. Routenberg, P.N. Wyrembak, D.B. Turner-Evans, A.D. Hamilton, D.A. LaVan, T.M. Fahmy, M.A. Reed, Label-free immunodetection with CMOS-compatible semiconducting nanowires, Nature 445 (2007) 519.
[28] H. Zhang, Z. Wang, S. Zhou, Simultaneous determination of nitrophenol isomers at the single-wall carbon nanotube compound conducting polymer film modified electrode, Science in China Series B 48 (2005) 177.
[29] L.X. Zeng, Q.F. Li, G.N. Chen, D.P. Tang, M.D. Wei, Metal platinum-wrapped mesoporous carbon for sensitive electrochemical immunosensing based on cyclodextrin functionalized graphene nanosheets, Electrochimica Acta 68 (2012) 158.
[30] D. Zhao, J. Feng, Q. Huo, N. Melosh, G. Fredrickson, B. Chmelka, G. Stucky, Triblock copolymer syntheses of mesoporous silica with periodic 50 to 300 angstrom pores, Science 279 (1998) 548.
[31] S. Jun, S. Joo, R. Ryoo, M. Kruk, M. Jaroniec, Z. Liu, T. Ohsuna, O. Terasaki, Synthesis of new, nanoporous carbon with hexagonally ordered mesostructure, Journal of the American Chemical Society 122 (2000) 10712.
[32] J.C. Ndamanisha, L.P. Guo, Ordered mesoporous carbon for electrochemical sensing: a review, Analytica Chimica Acta 747 (2012) 19.
[33] L. Li, B. Liang, F. Li, J. Shi, M. Mascini, Q. Lang, A. Liu, Co-immobilization of glucose oxidase and xylose dehydrogenase displayed whole cell on multiwalled carbon nanotube nanocomposite films modified electrode for simultaneous voltammetric detection of d-glucose and d-xylose, Biosensors and Bioelectronics 42 (2013) 156.
[34] Y.-e. Gu, Y. Zhang, F. Zhang, J. Wei, C. Wang, Y. Du, W. Ye, Investigation of photoelectrocatalytic activity of $Cu_2O$ nanoparticles for p-nitrophenol using rotating ring-disk electrode and application for electrocatalytic determination, Electrochimica Acta 56 (2010) 953.
[35] Y.-f. Hu, Z.-h. Zhang, H.-b. Zhang, L.-j. Luo, S.-z. Yao, Sensitive and selective imprinted electrochemical sensor for p-nitrophenol based on ZnO nanoparticles/carbon nanotubes doped chitosan film, Thin Solid Films 520 (2012) 5314.
[36] Y. Samet, D. Kraiem, R. Abdelhédi, Electropolymerization of phenol, o-nitrophenol and o-methoxyphenol on gold and carbon steel materials and their corrosion protection effects, Progress in Organic Coatings 69 (2010) 335.
[37] C. Zhou, Z. Liu, Y. Dong, D. Li, Electrochemical behavior of o-nitrophenol at hexagonal mesoporous silica modified carbon paste electrodes, Electroanalysis 21 (2009) 853.
[38] W. Huang, C. Yang, S. Zhang, Simultaneous determination of 2-nitrophenol and 4-nitrophenol based on the multi-wall carbon nanotubes Nafion-modified electrode, Analytical and Bioanalytical Chemistry 375 (2003) 703.
[39] R.S. Nicholson, I. Shain, Experimental verification of an ECE mechanism for the reduction of p-nitrosophenol, stationary electrode polarography using, Analytical Chemistry 37 (1965) 190.
[40] R.S. Nicholson, J.M. Wilson, M.L. Olmstead, Polarographic theory for an ECE mechanism application to reduction of p-nitrosophenol, Analytical Chemistry 38 (1966) 542.
[41] H. Yin, Q. Ma, Y. Zhou, S. Ai, L. Zhu, Electrochemical behavior and voltammetric determination of 4-aminophenol based on graphene–chitosan composite film modified glassy carbon electrode, Electrochimica Acta 55 (2010) 7102.
[42] L.-q. Luo, X.-l. Zou, Y.-p. Ding, Q.-S. Wu, Derivative voltammetric direct simultaneous determination of nitrophenol isomers at a carbon nanotube modified electrode, Sensors and Actuators, B 135 (2008) 61.
[43] Q. Shi, G. Diao, The electrocatalytical reduction of m-nitrophenol on palladium nanoparticles modified glassy carbon electrodes, Electrochimica Acta 58 (2011) 399.
[44] D.S. Silvester, A.J. Wain, L. Aldous, C. Hardacre, R.G. Compton, Electrochemical reduction of nitrobenzene and 4-nitrophenol in the room temperature ionic liquid $[C_4dmim][N(Tf)_2]$, Journal of Electroanalytical Chemistry 596 (2006) 131.